Effect of chain extender and water-quenching on the properties of poly(3- hydroxybutyrate-co-4-hydroxybutyrate) foams for its production by extrusion foaming

Heura Ventura[1], Ester Laguna-Gutiérrez[2], Miguel Angel Rodriguez-Perez[2], Mònica Ardanuy[1*]

[1] Departament d'Enginyeria Tèxtil i Paperera (DETiP), Universitat Politècnica de Catalunya (UPC)
C/Colom 11 - 08222 Terrassa, Barcelona, Spain

[2] Cellular Materials Laboratory (CellMat Lab), Condensed Matter Physics Department, Universidad de Valladolid (UVa)
Paseo Belén 4, Facultad de Ciencias - 47011, Valladolid, Spain

[*] Corresponding author: Mònica Ardanuy, e-mail: monica.ardanuy@upc.edu

Abstract

Bacterial polyesters such as polyhydroxyalkanoates (PHAs) are of great interest for a large number of applications both because of their properties and because they come from renewable resources, despite having a higher cost than commodity polymers. Their foaming—although it presents some difficulties—could be an option to increase their competitiveness. In this work, two strategies have been studied to enhance the poly(3-hydoxybutyrate-*co*-4-hydroxybutyrate) (P3HB4HB) foamability by extrusion foaming. The effect of the cooling system (water-quenching or air-cooling), chain extender (CE) addition and chemical blowing agent (CBA) amount were evaluated. Density, cellular morphology, mechanical and thermal properties were studied. Optimal density reduction was achieved with use of CE and 3–4 wt.% of CBA masterbatch. The most effective strategy on density reduction was the addition of CE, while the water quenching had only a slight influence on the samples in which CE was not present. CE addition decreased the viscosity and the degradation rate of the polymer, thus leading to lighter foams with larger cells but with equal or even slightly better resistance to compressive and tensile stress, in general terms.

Keywords: poly(3-hydoxybutyrate-*co*-4-hydroxybutyrate), biopolymer, chain extender, extrusion foaming, mechanical characterisation

1. Introduction

PHAs are a family of microbial biodegradable bacterial biopolyesters [1–3] that are obtained from renewable resources, and are of interest for a wide range of applications from packaging to biomedical industries [2,3]. However, due to its current high price compared with other commodity polymers, PHAs' commercial use is currently limited to those applications in which the biodegradability or biocompatibility properties are capable of outbalancing the cost of the PHA resin.

A possible strategy to reduce the amount of polymer required for a certain application, and therefore, the cost of the final good, is the weight reduction obtained from foaming the solid material leading to a foam with improved specific mechanical properties [4]. Nonetheless, the foaming of PHAs has some difficulties, since most PHAs are intrinsically difficult to foam because of a narrow processing window and a low melt strength, which leads to a tendency towards cell coalescence and collapse at high expansion [5].

Among all the foaming techniques, one of the most widely used is extrusion foaming due to its low cost for the production of continuous foams and high productivity. With this technique, blowing agents can be physical (PBAs) or chemical (CBAs). PHAs have already been foamed with super critical CO_2 gas as PBA [6], with exothermic CBAs such as azodicarbonamide (ADA) [5,7], or with more eco-friendly endothermic CBAs mainly based on sodium bicarbonate (SB) and citric acid [5,8,9]. The use of PBAs requires extruders with PBA-pumping systems and, in some cases, screws with special profiles, thus meaning that special processing machinery is necessary. Due to that, this study focuses on the use of CBAs, which allows its foam-processing in conventional extruder machines.

The aforementioned endothermic CBAs, which release CO_2 gas, have been shown to achieve lower density-PHA foams than exothermic CBAs such as ADA, which release N_2 gas [5]. Nevertheless, the use of endothermic CBAs has some drawbacks. The thermal decomposition of SB produces water in addition to CO_2, which can lead to an hydrolytic degradation of PHAs—an effect that is more noticeable at high processing temperatures [5,10–12] or large residence times [13] in which PHAs also suffer from thermal degradation. Both thermal and hydrolytic degradation of PHAs are caused by random chain scission, and hence, a decrease in the molecular weight is produced [10], which reduces not only the properties of the polymer but also its foamability. Therefore, both the CBA and the process itself adversely affect the resulting foam.

On the other hand, it is known that branched structures can enhance the melt strength and, therefore, the foamability of polymers. Epoxy-functionalised chain extenders (CEs) can be used to increase the molecular weight and melt viscosity, and also to improve the melt strength by means of chain branching and chain extension in other polymers [14]. The use of CEs for foamability improvement has already been proved in other biodegradable polyesters, such as PLA. In some cases, their addition increased the molecular weight, enhanced melt viscosity and improved the cellular structure by promoting the formation of a large amount of uniform small cells [15–18]. Furthermore, the use of CEs in PHAs has been reported to increase thermal stability, thus widening the processing window to improve sheet extrusion or foaming processes [19]. Nonetheless, to the authors' knowledge, only a few articles have focused on the influence of these CEs in the properties of PHAs; and even fewer have focused on the variation of cellular structure and mechanical properties of PHA foams due to CE addition.

Another proposal for improving PHA foamability when produced via extrusion foaming is water-quenching [5]. Wright and Frank [5] found an improvement in the cellular structure of

extruded PHA SB-blown foams when water-quenching post-extrusion was performed, since foams presented better cellular homogeneity and higher cell density. This was explained based on controlling the crystallinity due to the fast cooling rate produced by the water-quenching. Nevertheless, these authors did not study the effect of the use of a chain extender and no analysis of the effects on the mechanical properties was performed.

From the large family of PHAs, poly(3-hydroxybutyrate) (PHB) and its copolymers such as poly(3-hydroxybutyrate-*co*-3-hydroxyvalerate) (PHBV), poly(3-hydroxybutyrate-*co*-4-hydroxybutyrate) (P3HB4HB), or poly(3-hydroxybutyrate-*co*-hydroxyhexanoate) (PHBHHx) are the most widely studied. Regarding PHAs' foaming, the aforementioned research is mainly focused on PHBV and, in fewer cases, on PHBHHx. Nevertheless, to the authors' knowledge, none has focused on the PHB copolymer used in this study (P3HB4HB).

The aim of this study was to evaluate the combinations of the two strategies (water quenching and addition of chain extender) to enhance P3HB4HB extrusion foamability using an endothermic CBA, since their immediate application to the current processing technologies would be simple. The effects on the foamability of CBA content, chain extender addition and the cooling system were evaluated by means of cellular structure characterisation and analysis of the thermal and mechanical properties.

2. Experimental section

2.1. Materials

The poly(3-hydroxybutyrate-*co*-4-hydroxybutyrate) used for this research was Mirel P3001 (thermoforming grade, Metabolix Inc., USA). The chemical blowing agent (CBA) used was Hydrocerol BIH40E in masterbatch form (40 wt.% of CBA) from Clariant GmBH, Germany. Joncryl ADR-4368-C (FDA approved grade, kindly provided by BASF, Germany) was used as the chain extender (CE).

2.2. Samples preparation

Foamed samples were produced directly by extrusion foaming in a Collin Co-rotating Twin-screw Extruder ZK 25 T. PHA and CBA were previously dried at 50 ºC for 16 h in a P-Selecta Vacuum Drying Oven VacioTem TV. A reverse extrusion profile was used, linearly decreasing from 170 ºC in the hopper to 150 ºC in the die. The screw-speed was fixed to 70 rpm. The feeding and mass flow rates at these conditions were estimated to be around 71 ±3 g/min. The pressure measured at the die was in the range of 6.1 ±3 MPa. At the exit of the die (with a circular profile of 4-mm diameter), 50–60 specimens of each sample (with a length of ~20–25 cm) were collected. Half of the specimens were water-quenched in a water bath at 23 ±1 ºC after few seconds (5–10 s) of their exit through the die (referred to as W). The other specimens were air-cooled at room temperature (referred to as A). Sample cooling was done under no stress. After cooling, all the specimens were kept in standard conditions of temperature and relative humidity (23 ±2 ºC, 50 ±10% RH). Twelve different compositions were obtained by varying the CBA amount (six levels, from 0 to 5 wt.%), CE amount (two levels: 0 and 1 wt.%), and the cooling system used (air or water), as shown in Table 1.

Table 1. Composition and reference of the samples prepared (CBA=Chemical Blowing Agent; CE=Chain Extender; A=Air cooling; W=Water quenching)

Series	*Ref.*	*CBA*[1] (wt.%)	*CE* (wt.%)	*Cooling system*	*Series*	*Ref.*	*CBA*[1] (wt.%)	*CE* (wt.%)	*Cooling system*
0CE/A	0CBA-0CE/A	0	0	A	**0CE/W**	0CBA-0CE/W	0	0	W
	1CBA-0CE/A	1	0	A		1CBA-0CE/W	1	0	W
	2CBA-0CE/A	2	0	A		2CBA-0CE/W	2	0	W
	3CBA-0CE/A	3	0	A		3CBA-0CE/W	3	0	W
	4CBA-0CE/A	4	0	A		4CBA-0CE/W	4	0	W
	5CBA-0CE/A	5	0	A		5CBA-0CE/W	5	0	W
1CE/A	0CBA-1CE/A	0	1	A	**1CE/W**	0CBA-1CE/W	0	1	W
	1CBA-1CE/A	1	1	A		1CBA-1CE/W	1	1	W
	2CBA-1CE/A	2	1	A		2CBA-1CE/W	2	1	W
	3CBA-1CE/A	3	1	A		3CBA-1CE/W	3	1	W
	4CBA-1CE/A	4	1	A		4CBA-1CE/W	4	1	W
	5CBA-1CE/A	5	1	A		5CBA-1CE/W	5	1	W

[1] CBA content refers to wt.% of the masterbatch.

2.3. Characterisation methods

2.3.1. Rheological characterisation

For the evaluation of the effect of CE addition, a rheological characterisation using oscillatory shear rheometry was performed. In order to compare samples with the same thermal history, P3HB4HB and the mixture (P3HB4HB and 1 wt.% of CE) were extruded following the processing conditions described in section 2.2. After the extrusion, the samples were collected, air-cooled and dried for 12 h at 50 ºC under vacuum. Then, the samples obtained were moulded into 1 mm-thick discs at 175 ºC under 10,000 kg for 3 min in a Remtex Hot Plate Press. The assays were performed in a TA Instruments Rheometer AR 2000 EX, equipped with electrically heated parallel plates of 25 mm of diameter. The gap was set to 1 mm. The time-sweep was performed with an angular frequency of 1 rad/s and a fixed strain of 2% at a temperature of 165 ºC, which was in the linear viscoelastic regime. Since the objective was to study the degradation rate of the two samples, the atmosphere used was air instead of nitrogen, for a better simulation of the processing conditions.

2.3.2. Density

Density was determined by the water-displacement method, based on Archimedes' principle, obtaining an average value from three measurements. Relative density (ρ_{rel})—defined as the ratio between the foam's density and the solid's density—was also calculated.

2.3.3. Open-cell content

The open-cell content (f) was determined using a Micromeritics Gas Pycnometer AccuPyc II 1340 with nitrogen gas at 13.44 MPa and equilibration rate at $6.89 \cdot 10^{-5}$ MPa, by means of Eq. 1:

$$f = \frac{V_f - V_q}{V_f\left(1 - \frac{\rho_f}{\rho_s}\right)} \quad (1)$$

where V_f is the external volume of the tested sample (*i.e.* volume determined by the water-displacement method), V_q corresponds to the volume of the solid plus the gas volume of the unconnected cells (*i.e.* pycnometric volume), ρ_f is the foam's density, and ρ_s is the density of the solid phase (ρ_s = 1290 kg/m^3).

2.3.4. Characterisation of the cellular structure

For the characterisation of cellular structure, SEM images of fragile fractures were taken in a JEOL Scanning Electron Microscope JSM 820. Cellular structure analysis was performed using only images of the centre of the specimens. A user-interactive image analysis adaptation of the ASTM D3576-04 method was used [20]. Cell size (mean cell diameter) and cell density (per solid volume unit, N_0) were determined in section and transversal directions from 100–150 cells.

2.3.5. Differential scanning calorimetry

The differential scanning calorimetry (DSC) data were recorded on a Mettler DSC-862. A three-cycle DSC was performed under nitrogen flow of 60 mL/min: first heating cycle from -40 ºC to 200 ºC at 10 ºC/min with 3 min of annealing at 200 ºC; cooling cycle from 200 ºC to -40 ºC at 20 ºC/min; second heating cycle from -40 ºC to 200 ºC at 10 ºC/min. Melting temperatures (T_m) and crystallisation temperatures (T_c) were obtained as the maximum of the peaks from the endothermic and exothermic curves, respectively. Crystallinity percentage (χ) of all samples was estimated from melting enthalpy (ΔH_m) and crystallisation enthalpy (ΔH_c) according to Eq. 2:

$$\chi = \frac{\Delta H}{w \cdot \Delta H^0} \quad (2)$$

where w is the weight fraction of P3HB4HB in each case, ΔH is the heat at the melting or crystallisation peak, and ΔH^0 is the heat of fusion or crystallisation of 100% crystalline PHB, which is considered to be 146 J/g [21].

2.3.6. Compression tests

Compression tests were performed in an Instron Universal Testing Machine 5.500R6025. Six specimens of each sample were cut at a height (h) of around 5 mm, resulting in cylindrical specimens with parallel sides with a diameter/height ratio of 0.75. The tests were performed at a speed of h/10 mm/min (~0.5 mm/min) up to a strain of the 70%. Values of stress at 25% and 50% of the strain ($\sigma_{25\%}$ and $\sigma_{50\%}$, respectively) and the collapse stress at the plateau (σ_{pl}) were obtained from the curves for each specimen.

2.3.7. Tensile tests

Tensile tests were performed in an Instron Universal Testing Machine 5.500R6025 following ISO527 1A standard. Five no-standard-shaped specimens of each sample were tested. The cylindrical extrudate specimens were first cut to a length of 15 cm and then the sectional area was calculated in order to adjust each test result with the corresponding specimen. Mean values of maximum stress (σ_{max}) and ultimate tensile strength (σ_{UTS}) were calculated. A high scatter of the maximum strain data was observed, which is related to the brittleness of the samples; therefore, the data related to the strain was not considered.

2.3.8. Charpy impact tests

Charpy impact tests for comparative purposes were performed in a Frank Charpy Impact Tester 53.566, with a 4 J hammer and an anvil distance of 39 mm. Ten specimens of each sample, cut to a length of 50 mm, were tested. Energy values were corrected, taking into account the sectional area of each specimen.

3. Results

3.1. Rheological characterisation

The complex viscosity versus time is presented in Figure 1. Initial complex viscosity values were 2192 Pa·s for the neat polymer and 1638 Pa·s for the polymer with CE. This first viscosity data reveals that the addition of CE produces a decrease in the complex viscosity, which is relevant to explain the cellular morphology and will be described in section 3.3.

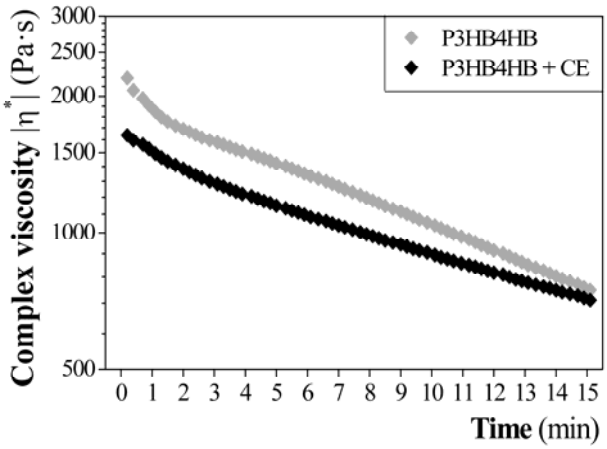

Figure 1. Complex viscosity against time.

Moreover, complex viscosity is also related to the degradation of the polymer. As can be seen in Figure 1, the most dramatic differences were revealed in the first minutes. For instance, after 2 min, the complex viscosity modulus of the neat polymer decreased 23%, while for the polymer with CE, the decrease was of 15%. This is related to a lower degradation rate when the CE is added. It has to be taken into account that the residence time of the material in the extruder during the foaming process was around 2–3 minutes. Therefore, although the CE addition produced a decrease in viscosity, the degradation rate was also reduced, thus leading to a less degraded polymer with expected better properties.

3.2. Density

Density values are shown in Figure 2. As expected, increasing amounts of CBA led to lower densities. Density values of near 750 kg/m^3 could be obtained with the addition of 3 wt.% CBA and 1 wt.% of CE.

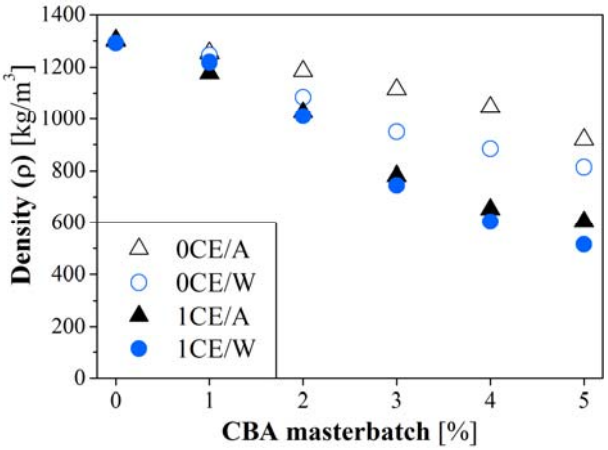

Figure 2. Density against CBA amount.

For the 0CE series (without chain extender: cooled in air – △ – or water – ○ –), an almost linear reduction in the density was observed. Since the water-quenching (○) produced faster solidification with lower contraction, and samples without the chain extender achieved lower densities with this cooling system. However, for the 1CE series (with chain extender: ▲ and ●), the differences due to the cooling system were negligible. The largest decrease in density was observed for CBA contents of 3 wt.% or higher when the CE was used. As aforementioned, the addition of CE produced a reduction on the viscosity, thus leading to higher expansion rates as will be discussed in section 3.2. Moreover, CE addition also reduced the degradation rate of the polymer, what could have led to a less degraded polymer present in the cell walls, thus leading to a better stability.

In the literature, the chain extender was presumed to enhance the polymer conditions for foaming, such as increased polymer viscosity, molecular weight or melt strength [18,19,22,23]. Although in this study a reduction in viscosity was observed as a consequence

of the CE addition, other properties such as melt strength or molecular weight could have been improved, thus intensifying the effect of the decrease in degradation previously discussed.

3.3. Cellular morphology

In general terms, the P3HB4HB foams of this study presented closed-cell structures with more regular pores in the inner part that tended to reduce in size and to lose the apparent isotropy when approaching the foam skin. However, some coalescence was observed. Foams with high CBA content showed coalescence in the inner part, where the heat was easily retained. In this sense, significant amounts of connected pores were observed in some cases. 4CBA-1CE/W 5CBA-1CE/A and 5CBA-1CE/W samples presented 15%, 27% and 62% of open-cell content, respectively, while negligible open-cell content of 6% or lower was found in the rest of the samples. Figure 3 shows cellular structure of sample 5CBA-1CE/W, which presented massive coalescence in the centre and some irregularities in the skin due to the collapse, thus explaining the high open-cell content of 62%.

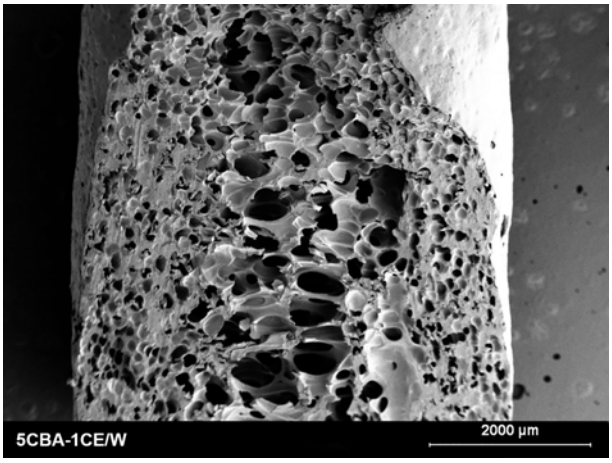

Figure 3. SEM image of transversal (bias) fracture of specimen 5CBA-1CE/W showing a poor cellular structure in the central area.

Moreover, samples containing the chain extender (corresponding to the higher expansions) showed acceptable cellular structures up to the addition of 4% of CBA. Further increases in

CBA content led to large coalescence in the centre of the samples as well as very irregular surfaces. According to the literature, a large amount of soluble gas would have been translated into high cell density, but at certain point the nucleated cells would have reached their maximum growth, and a further increase in the blowing agent would have led to coalescence and collapse of the cells [5,7,16].

The evolution of cellular structure for the four series when increasing CBA content can be observed in Figure 4. The cellular morphologies are in accordance with the density results mentioned previously.

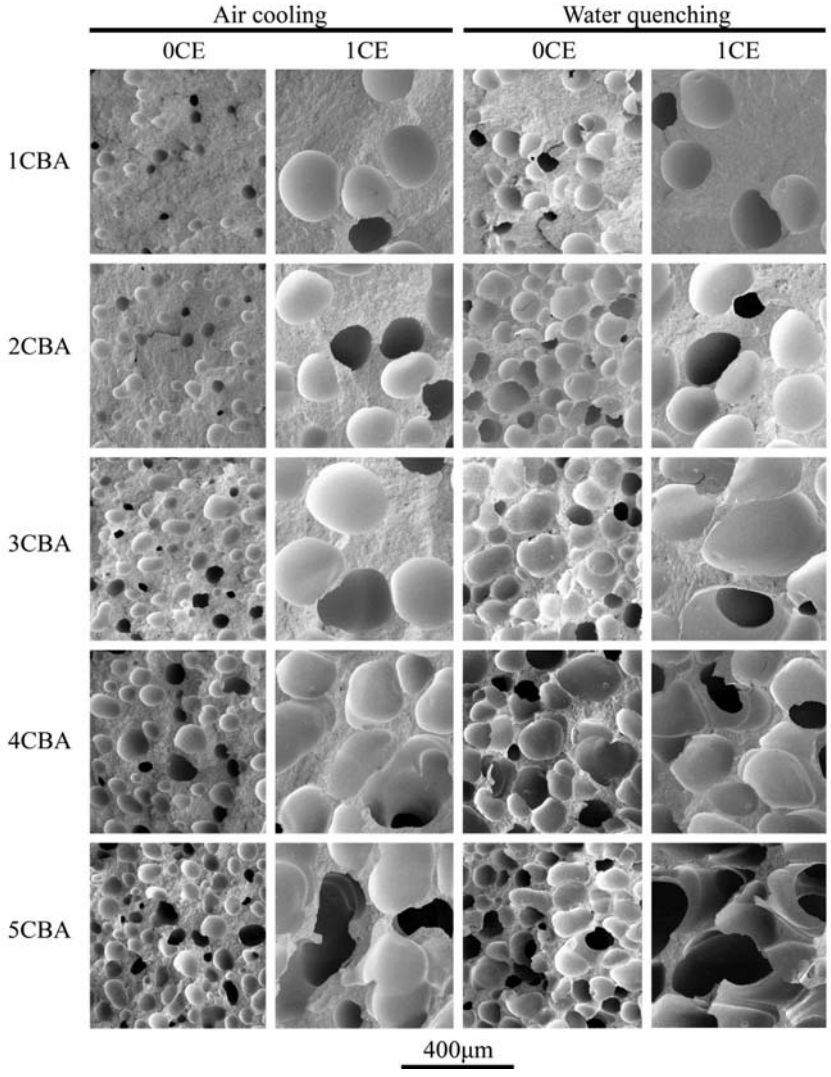

Figure 4. SEM images showing the evolution of the cellular structure in the samples section when increasing CBA content. (Magnification: 50X).

The data from the cellular structure analysis, in transversal and section directions, is presented in Figure 5. In general terms, the 0CE series presented larger cell densities (10^5–10^6 cells/cm^3) and smaller pores with diameters between 50–80 μm; and the 1CE series presented lower cell densities (10^4–10^5 cells/cm^3) with cells three-times larger than the 0CE series, of a diameter between 150–200 μm. Cell density (N_0) initially showed a fast growth with increasing CBA content in each series. Further narrowing or even recession of this trend was produced due to cell growth, coarsening and later coalescence.

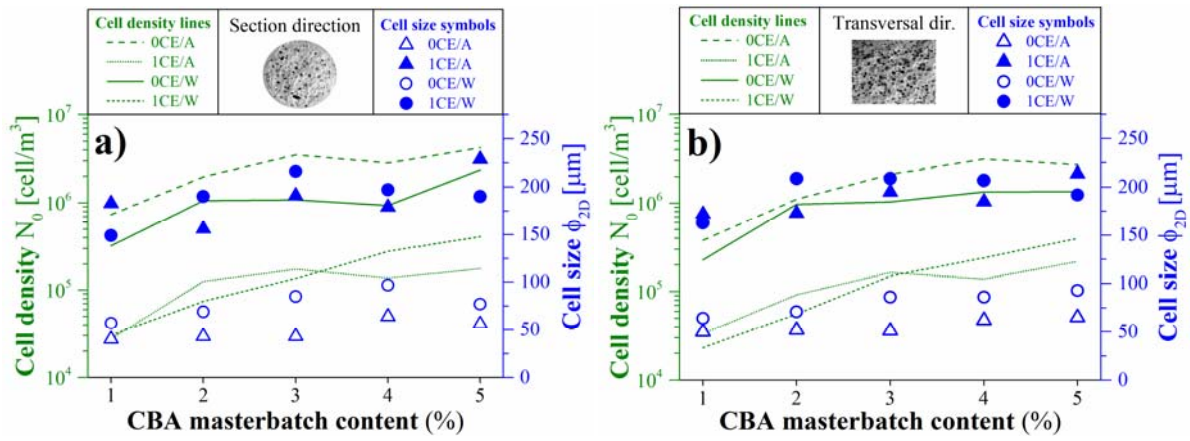

Figure 5. Graphic summary of the cellular structure analysis in the a) section direction and b) transversal direction, containing the cell density and cell size evolution with increasing the CBA.

On the one hand, the effect of the cooling system was observed in the cell size for the 0CE series, although it was not significant in the cell size of the 1CE series. The 0CE series presented cell sizes that were on average 50% larger in the water-quenched samples when compared to the air-cooled samples, thus explaining the slightly lower densities (see Figure 2). Shrinkage of the specimens was clearly observed during cooling in the air-cooled samples, which could lead to the differences observed in the cell size. However, differences in the cell size due to the cooling system were not relevant for the 1CE series. Moreover, similar trends in cell density evolution (of the 0CE series on one side, and of the 1CE series on the other) revealed similar cell formation and growing regardless of the cooling system used.

On the other hand, the addition of CE led to coarser cellular structures. The cell growth process is known to be related to the viscosity of the polymer melt [24], since low viscosity values favour the cell growth rate. Therefore, the lower initial complex viscosity observed for the 1CE series (see section 3.1) enhanced the cell growth rate, leading to more expanded foams with larger cells, as observed in Figures 2, 4 and 5. Moreover, the addition of CE also produced a decrease in the crystallisation temperature (see section 3.4.2), leading to a slower solidification of the foams. Therefore, a prolonged evolution of the cellular structure in terms of coalescence, coarsening and collapse took place, thus also promoting the coarser structures observed in Figure 4.

3.4. Thermal behaviour analysis

3.4.1. Crystallinity degree

In the first heating cycle (χ_m), the values of crystallinity degree obtained from all series showed a rising trend with decreasing relative density (Figure 6a). This general increase could be attributed to differences in the thermal properties of the foamed samples. In general terms, the reduction of density is translated into a decrease in the thermal conductivity [25], and thus to larger times at high temperature. Therefore, the heat retention enhanced the crystal formation, thus explaining the increasing trend with the decrease of the density. Moreover, as shown in Figure 6a, the air-cooled series (△ and ▲) presented slightly higher χ_m values than water-quenched series (○ and ●) in the first heating cycle, as expected, due to lower cooling rates [26]. However, once the sample is completely melted (at the end of the first heating cycle), the cellular structure is lost, thus levelling the thermal behaviour of all specimens. Thus, the following cycles presented scattered and more flat trends, as shown for the crystallinity of the second heating cycle in Figure 6b.

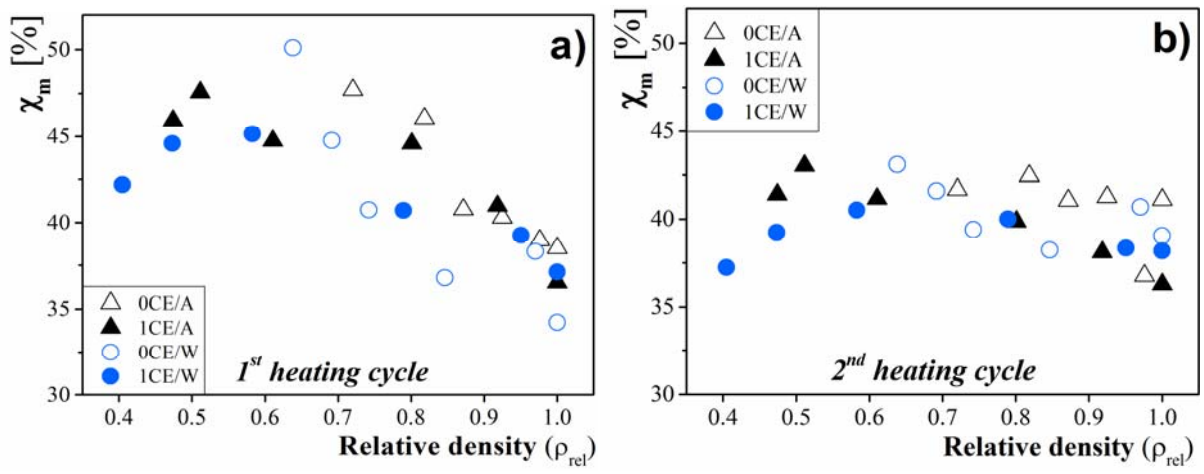

Figure 6. χ_m percentages for the a) first heating cycle and b) second heating cycle against relative density.

The addition of CE had no clear effect on the crystallinity, since χ_m values of the 1CE-series where over those of the 0CE-series, as can be seen in Figure 6. Nonetheless, in the literature, Pilla et al. reported a reduction in χ from around 10% in talc-filled PLA foams due to the addition of CE [15], and Ludwiczak and Kozlowski reported, among other effects, even larger reductions in the crystallinity percentage with increased CE in PLA foams [18]. These authors attributed this reduction to the formation of non-linear molecules or branched chains, which mainly difficult the packing of the chains, thus inhibiting the crystal formation. However, the interaction between the P3HB4HB and the chain extender could have been different from the PLA system studied in the literature. Here, the CE could have played only a minor role balancing or counteracting the thermal degradation, thus giving chains of similar properties that would not reveal large differences in chain packing, as in the other studies.

3.4.2. Melting and crystallisation temperatures

With regard to the DSC heating curves, a complex melting behaviour was observed (see Figure 7), which is consistent with the literature [26–29]. The DSC curves for the first heating cycle presented high dependence on the processing conditions (Figure 7a) and the CBA content (Figure 7b, showing the results for the 1CE/A-series as an example).

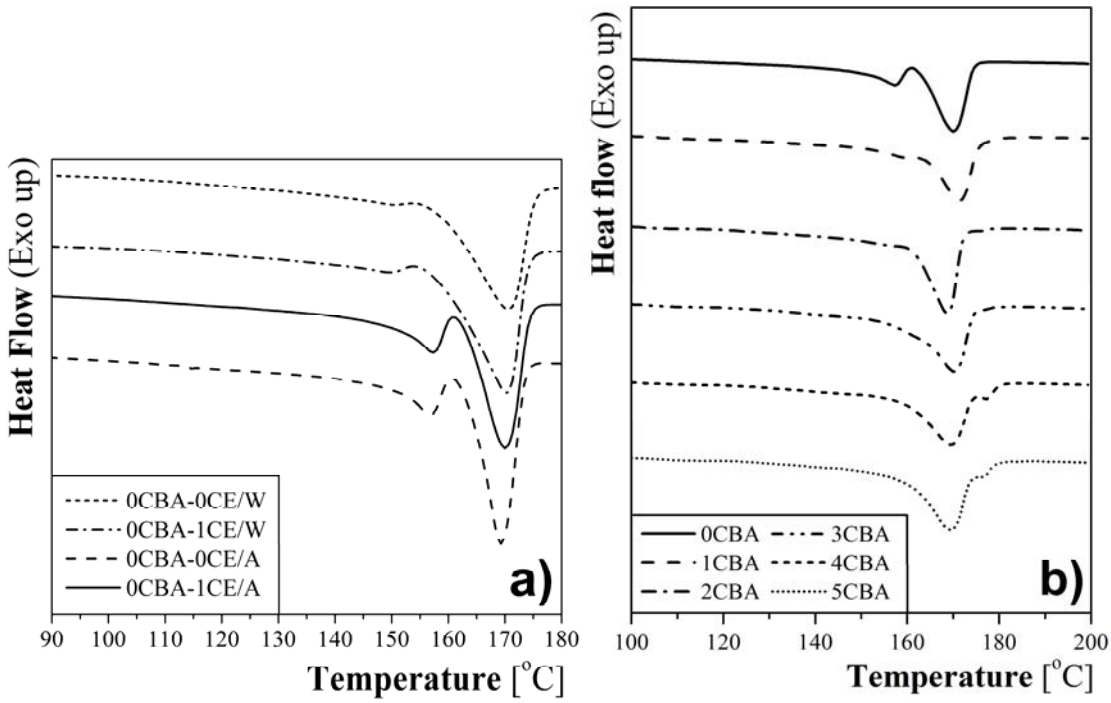

Figure 7. DSC first heating cycle-curves comparison for a) 0CBA samples; b) 1CE/A-series with increasing CBA contents from top to bottom.

However, in the second heating cycle where all samples were affected by the same thermal history, small variations due to the addition of CE were observed, since the melting peaks were observed at a temperature of 2–3 ºC lower compared to the 0CE series. Thus could be associated with the formation of less stable or thicker crystals when the CE is added.

With respect to the maximum crystallisation temperatures (T_c) obtained in the cooling cycle, no differences associated with the CBA amount or cooling system were detected. However, DSC revealed a T_c reduction from 105.4 ±0.2 ºC to 99.9 ±0.6 ºC due to the addition of the CE. This means that the formation of crystals in the series with CE is slower since it needs to reach lower temperatures. This crystallisation delay, due to CE addition, is consistent with the literature [18,19]. For instance, Duangphet et al. reported lower crystallisation temperatures and a slight decrease in the enthalpies of crystallisation for increasing amounts of Joncryl in PHBV [19].

3.5. Mechanical properties

Compression, tensile and impact tests were performed in order to characterise mechanical properties of the obtained foams. Relative properties were plotted against relative density, and the data were fitted to the scaling law using Eq. 3, with the purpose to guide the eye and ease the comparison of the results.

$$\frac{\text{Foam property}}{\text{Solid property}} = C \cdot \left(\frac{\rho_{foam}}{\rho_{solid}} \right)^{n} \quad (3)$$

As expected, density reduction was obtained at the expense of reducing the mechanical properties. The mechanical properties of the foams largely depend on the foam's density, but also on the properties of the solid material from which the cell walls are made [30]. Therefore, the less degraded is the polymer, the better mechanical properties of the foam are expected.

As a reference, the properties of all unfoamed samples (0 wt.% content of CBA) were similar: for compression testing, σ_{pl} = 39.3 ±0.8 MPa, $\sigma_{25\%}$ = 44.6 ±1.8 MPa and $\sigma_{50\%}$ = 61.4 ±3.7 MPa; and for tensile testing, σ_{max} = 25.4 ±0.9 MPa and σ_{UTS} = 23.5 ±1.6 MPa.

3.5.1. Compression testing results

Compression-test curves of all obtained foams show the typical behaviour observed for cellular materials: an initial elastic deformation, in which the cell walls suffer from elastic bending and cell walls suffer some stretching; this is followed by a change in the slope that marks a plateau, which is associated with the collapse of cell walls of the foam; and finally, the progressive densification associated with the compression of the solid matrix, since cell walls have completely collapsed, and hence, cellular structure is lost.

The tangent method was used in σ_{pl} calculations. Samples corresponding to the lower densities (up to 918 kg/m^3) presented an elasto-plastic behaviour with a clear plateau [30], probably because the thinner cell walls and higher crystallinity observed in more expanded foams resulted in more brittleness. The rest of the samples—*i.e.* those corresponding to the

higher densities (≥949 kg/m^3) with thicker cell walls and lower crystallinity—presented a change in the slope, but not a clear plateau. Each series presented a progressive reduction of the compression curves with increasing CBA content (example in Figure 8) as a consequence of the density reduction.

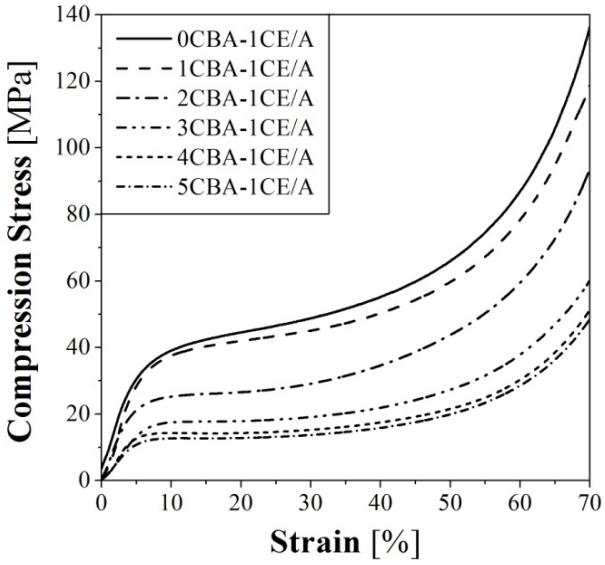

Figure 8. Compression curves for 1CE/A series, showing the evolution of the behaviour when increasing the CBA amount (average standard deviations were around 8%).

The plot of the measured relative properties against relative density is presented in Figure 9. A slightly better behaviour of the 1CE/A series can be observed in the compression stress at the plateau (Figure 9a). However, for larger deformations (at 25% of the strain, Figure 9b, and at 50% of the strain, Figure 9c), the mechanical behaviour of all samples was similar, giving superposed curves with small differences that are not forceful given the high standard deviations obtained.

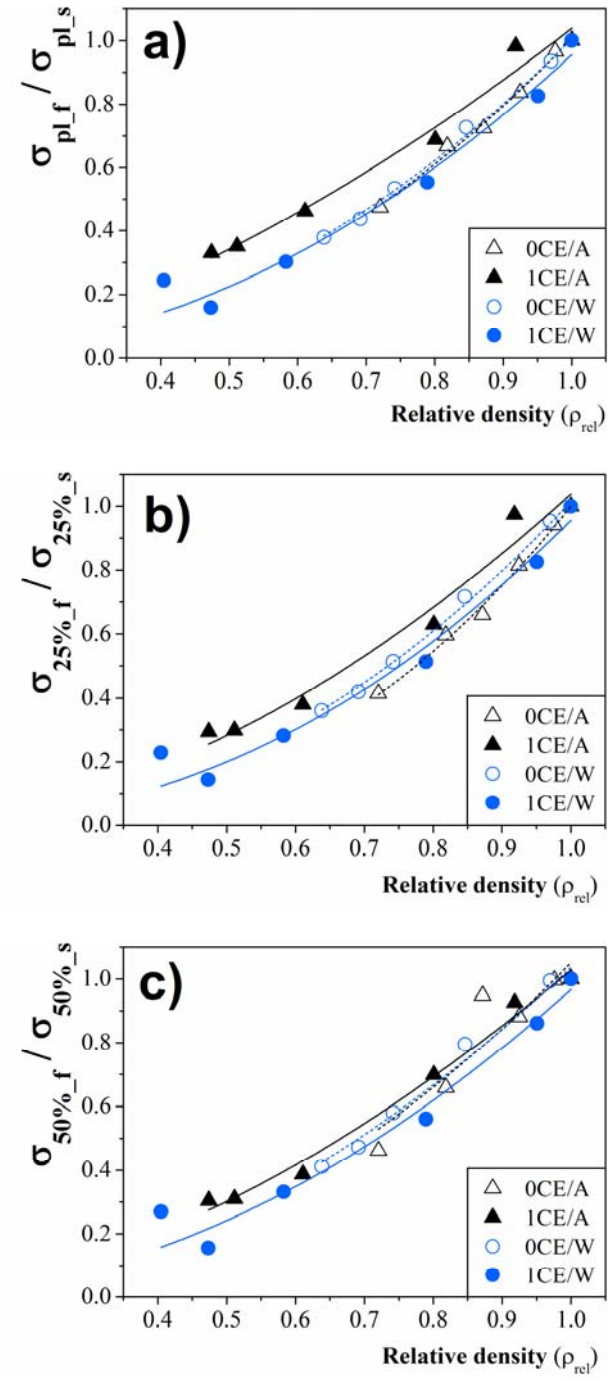

Figure 9. Representation of relative compression properties: a) relative stress at the plateau σ_{pl}; b) relative stress at 25% of strain $\sigma_{25\%}$; c) relative stress at 50% of strain $\sigma_{50\%}$; against relative density. Relative refers to the properties of the foam versus the properties of the solid. The fitting lines (which follow the scaling law) have been included to guide the eye.

In general terms, the best results in compression mode were obtained with the 1CE/A series, which gave slightly better performance, especially in σ_{pl}. Here, the CE reduced the degradation rate of the polymer and hence, low densities could be achieved. Moreover, a high

crystallinity degree was reached due to the slow air-cooling. As previously shown in Figure 6, the 1CE/A series presented a good χ/ρ ratio that was higher than the water-quenched samples. Therefore, the combined effects of the CE and crystallinity overcame the loss of properties due to the cellular structure, thus explaining the better results. The other series presented very similar trends, regardless of the cooling system or the CE addition, thus pointing to the complexity of the system being studied.

3.5.2. Tensile testing results

Tensile properties decreased when increasing the expansion ratios, as expected, given the reduction of the effective section because of the foam's structure. Maximum stress (σ_{max}) and ultimate tensile strength values (σ_{UTS}) were recorded, and the SD was 9% and 10%, respectively. Once again, relative properties were represented against relative density (Figure 10).

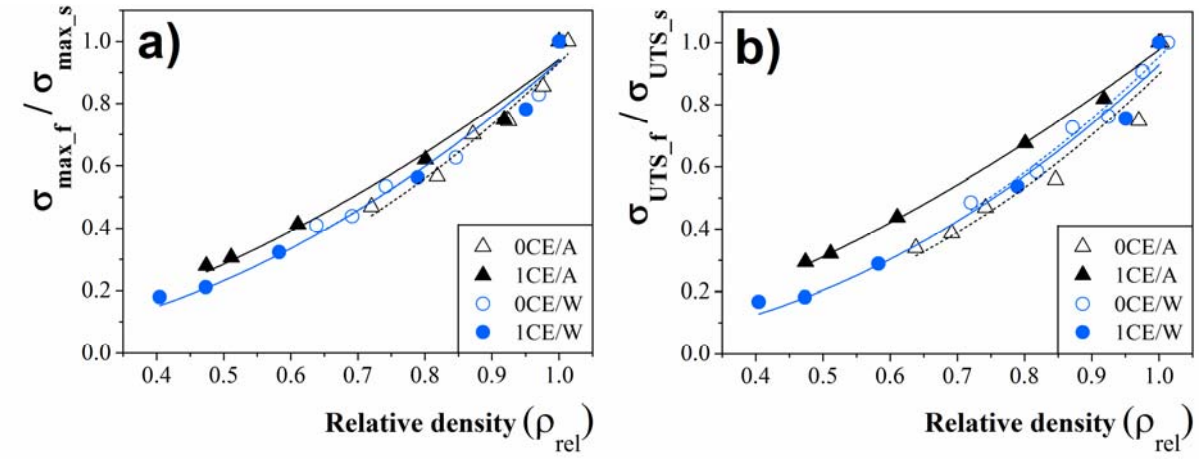

Figure 10. Representation of relative tensile properties: a) relative maximum strength σ_{max}; b) relative ultimate tensile strength σ_{UTS}; against relative density. Relative refers to the properties of the foam versus the properties of the solid. The fitting lines (which follow the scaling law) have been included to guide the eye.

Considering the high deviations obtained in the tensile tests, the curves in Figure 10 show very similar behaviours under tensile modes for all the samples, thus the strategies used

produced no improvements nor deteriorations in mechanical properties beyond those expected due to the density's reduction. However, the 1CE/A series presented slightly better results for the ultimate tensile strength (Figure 10b), associated with a better preservation of the polymer via CE addition. Once again, a good balance between the lower degradation of the polymer and the high crystallinity values achieved could explain the slightly better results, although the cellular structure is not favourable for such a behaviour.

3.5.3. Impact testing results

In Figure 11, a comparison of the results of the impact against density is shown (error bars correspond to standard deviations values). Taking into account the high deviations, the observed results were within the expected range of the general impact properties of foams. All samples showed very similar behaviour regardless of the CE addition and the cooling system.

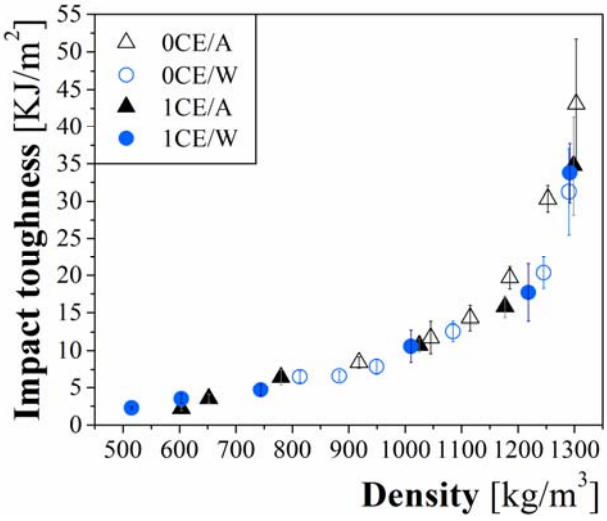

Figure 11. Impact toughness against density.

In addition to this, the density was the most significant factor in the impact behaviour of the samples, as expected. The addition of only 1 wt.% CBA reduced the density around ~3% and ~8%, causing a decrease of 30% and 50% in the impact toughness of the 0CE and 1CE series, respectively. However, further additions of CBA led to less severe drops in impact toughness.

The high standard deviation values impede determining whether other factors, such as crystallinity, have any effect on the impact properties, as might be expected.

Conclusions

In this study, PHA foams were successfully achieved by extrusion foaming with an endothermic CBA. Effects of the CBA content, as well as the effects of the two strategies (CE-addition and water cooling) were evaluated.

The results revealed a very complex system given, on the one hand, the intrinsic complexity of the polymer under study. On the other hand, opposing processes occurred simultaneously, some of them (such as hydrolytic degradation, CBA decomposition and cellular structure evolution, among others) impoverishing and some of them (such as chain extension and/or branching, and crystallinity variation) enhancing the foam's properties.

Regarding the CE addition, the strategy was more effective, regardless of the cooling system used, since it led to lower densities without producing a negative effect on the mechanical properties (the reduction observed in the mechanical properties was in the range of what was expected due to the decrease in the density). CE addition led to lower viscosity and coarser cellular morphologies, but at the same time, prevented the polymer degradation (by reducing the degradation rate), thus leading to a less degraded polymer with better properties.

The water-cooling strategy enhanced the density reduction only when the chain extender was not used, and could not reach the effectiveness of the CE addition.

No clear synergies were observed when combining both strategies.

The mechanical properties were strongly affected by the density reduction, as expected, and were similar for all samples; however, slightly better behaviour was observed for the 1CE/A series. In this sense, it can be concluded that optimal results were obtained with the use of CE (1 wt.%), 3–4 wt.% CBA content, and air cooling, since a balance between the mechanical properties and the density reduction could be achieved here.

Acknowledgements

The authors would like to acknowledge MECD (Government of Spain) for the fellowship FPU12/05869 to H. Ventura and the PIRTU contract of E. Laguna-Gutiérrez by Junta of Castilla and Leon (EDU/289/2011) and co-financed by the European Social Fund. Financial assistance from MINECO (Government of Spain) and FEDER PROGRAM (BIA2014-59399-R and MAT 2012-34901) and the Junta of Castile and Leon (VA035U13) is also gratefully acknowledged.

References

[1] B. Laycock, P. Halley, S. Pratt, A. Werker, P. Lant, The chemomechanical properties of microbial polyhydroxyalkanoates, Prog. Polym. Sci. 39 (2014) 397–442. doi:10.1016/j.progpolymsci.2013.06.008.

[2] C.S.K. Reddy, R. Ghai, Rashmi, V.C. Kalia, Polyhydroxyalkanoates: An overview, Bioresour. Technol. 87 (2003) 137–146. doi:10.1016/S0960-8524(02)00212-2.

[3] R.A. Shanks, A. Hodzic, S. Wong, Thermoplastic biopolyester natural fiber composites, J. Appl. Polym. Sci. 91 (2004) 2114–2121. doi:10.1002/app.13289.

[4] M.A. Rodríguez-Pérez, Crosslinked Polyolefin Foams: Production, Structure, Properties, and Applications, in: Crosslink. Mater. Sci., Springer Berlin Heidelberg, Berlin, Heidelberg, 2005: pp. 97–126. doi:10.1007/b136244.

[5] Z.C. Wright, C.W. Frank, Increasing cell homogeneity of semicrystalline, biodegradable polymer foams with a narrow processing window via rapid quenching, Polym. Eng. Sci. 54 (2014) 2877–2886. doi:10.1002/pen.23847.

[6] N. Le Moigne, M. Sauceau, M. Benyakhlef, R. Jemai, J.-C. Benezet, E. Rodier, et al., Foaming of poly(3-hydroxybutyrate-co-3-hydroxyvalerate)/organo-clays nano-biocomposites by a continuous supercritical CO2 assisted extrusion process, Eur. Polym. J. 61 (2014) 157–171. doi:10.1016/j.eurpolymj.2014.10.008.

[7] Q. Liao, A. Tsui, S. Billington, C.W. Frank, Extruded foams from microbial poly(3-hydroxybutyrate-co-3-hydroxyvalerate) and its blends with cellulose acetate butyrate, Polym. Eng. Sci. 52 (2012) 1495–1508. doi:10.1002/pen.23087.

[8] A.H. Behravesh, C.B. Park, L.K. Cheung, R.D. Venter, Extrusion of polypropylene foams with hydrocerol and isopentane, J. Eng. Appl. Sci. 2 (1996) 1862–1867. doi:10.1002/vnl.10153.

[9] D. Szegda, S. Daungphet, J. Song, K. Tarverdi, Extrusion foaming and rheology of PHBV, in: 8th Int. Conf. Foam Mater. Technol., 2010: pp. 6–11.

[10] H. Verhoogt, B. a Ramsay, B.D. Favis, J. a Ramsay, The influence of thermal history on the properties of poly(3-hydroxybutyrate-co-12%-3-hydroxyvalerate), J. Appl. Polym. Sci. 61 (1996) 87–96. doi:10.1002/(SICI)1097-4628(19960705)61:1<87::AID-APP10>3.0.CO;2-X.

[11] I. Chodak, Polyhydroxyalkanoates: Origin, Properties and Applications, in: M.N. Belgacem, A. Gandini (Eds.), Monomers, Polym. Compos. from Renew. Resour., Elsevier, 2008: pp. 451–477. doi:10.1016/B978-0-08-045316-3.00022-3.

[12] L. Cabedo, D. Plackett, E. Giménez, J.M. Lagarón, Studying the degradation of polyhydroxybutyrate-co-valerate during processing with clay-based nanofillers, J. Appl. Polym. Sci. 112 (2009) 3669–3676. doi:10.1002/app.29945.

[13] M. Yamaguchi, K. Arakawa, Effect of thermal degradation on rheological properties for poly(3-hydroxybutyrate), Eur. Polym. J. 42 (2006) 1479–1486. doi:10.1016/j.eurpolymj.2006.01.022.

[14] M. Villalobos, a. Awojulu, T. Greeley, G. Turco, G. Deeter, Oligomeric chain extenders for economic reprocessing and recycling of condensation plastics, Energy. 31 (2006) 3227–3234. doi:10.1016/j.energy.2006.03.026.

[15] S. Pilla, S.G. Kim, G.K. Auer, S. Gong, C.B. Park, Microcellular extrusion-foaming of polylactide with chain-extender, Polym. Eng. Sci. 49 (2009) 1653–1660. doi:10.1002/pen.21385.

[16] L.M. Matuana, O. Faruk, C. a. Diaz, Cell morphology of extrusion foamed poly(lactic acid) using endothermic chemical foaming agent, Bioresour. Technol. 100 (2009) 5947–5954. doi:10.1016/j.biortech.2009.06.063.

[17] J. Wang, W. Zhu, H. Zhang, C.B. Park, Continuous processing of low-density, microcellular poly(lactic acid) foams with controlled cell morphology and crystallinity, Chem. Eng. Sci. 75 (2012) 390–399. doi:10.1016/j.ces.2012.02.051.

[18] J. Ludwiczak, M. Kozlowski, Foaming of Polylactide in the Presence of Chain Extender, J. Polym. Environ. 23 (2015) 137–142. doi:10.1007/s10924-014-0658-7.

[19] S. Duangphet, D. Szegda, J. Song, K. Tarverdi, The Effect of Chain Extender on Poly(3-hydroxybutyrate-co-3-hydroxyvalerate): Thermal Degradation, Crystallization, and Rheological Behaviours, J. Polym. Environ. 22 (2013) 1–8. doi:10.1007/s10924-012-0568-5.

[20] J. Pinto, E. Solorzano, M. a. Rodriguez-Perez, J. a. de Saja, Characterization of the cellular structure based on user-interactive image analysis procedures, J. Cell. Plast. 49 (2013) 555–575. doi:10.1177/0021955X13503847.

[21] P.J. Barham, A. Keller, E.L. Otun, P.A. Holmes, Crystallization and morphology of a bacterial thermoplastic: poly-3-hydroxybutyrate, J. Mater. Sci. 19 (1984) 2781–2794. doi:10.1007/BF01026954.

[22] Q. Meng, M.-C. Heuzey, P.J. Carreau, Control of thermal degradation of polylactide/clay nanocomposites during melt processing by chain extension reaction, Polym. Degrad. Stab. 97 (2012) 2010–2020. doi:10.1016/j.polymdegradstab.2012.01.030.

[23] N. Najafi, M.C. Heuzey, P.J. Carreau, P.M. Wood-Adams, Control of thermal degradation of polylactide (PLA)-clay nanocomposites using chain extenders, Polym. Degrad. Stab. 97 (2012) 554–565. doi:10.1016/j.polymdegradstab.2012.01.016.

[24] R. Liao, W. Yu, C. Zhou, Rheological control in foaming polymeric materials: I. Amorphous polymers, Polymer (Guildf). 51 (2010) 568–580. doi:10.1016/j.polymer.2009.11.063.

[25] O.A. Almanza, M.A. Rodriguez-Perez, J.A. De Saja, The thermal conductivity of polyethylene foams manufactured by a nitrogen solution process, Cell. Polym. 18 (n.d.) 385–401. http://cat.inist.fr/?aModele=afficheN&cpsidt=1316288 (accessed July 18, 2016).

[26] L.M.W.K. Gunaratne, R. a. Shanks, G. Amarasinghe, Thermal history effects on crystallisation and melting of poly(3-hydroxybutyrate), Thermochim. Acta. 423 (2004) 127–135. doi:10.1016/j.tca.2004.05.003.

[27] H. Mitomo, Y. Doi, Lamellar thickening and cocrystallization of poly(hydroxyalkanoate)s on annealing, Int. J. Biol. Macromol. 25 (1999) 201–205. doi:10.1016/S0141-8130(99)00035-5.

[28] R.M.R. Wellen, M.S. Rabello, G.J.M. Fechine, E.L. Canedo, The melting behaviour of poly(3-

hydroxybutyrate) by DSC. Reproducibility study, Polym. Test. 32 (2013) 215–220. doi:10.1016/j.polymertesting.2012.11.001.

[29] H. Mitomo, P.J. Barham, A. Keller, Crystallization and Morphology of Poly(β-hydroxybutyrate) and its Copolymer, Polym. J. 19 (1987) 1241–1253. doi:10.1295/polymj.19.1241.

[30] L.J. Gibson, M.F. Ashby, Cellular Solids: Structure and properties, 2nd ed., Cambridge University Press, Cambridge, 1999.

Figure captions

Figure 1. Complex viscosity against time.

Figure 2. Density against CBA amount.

Figure 3. SEM image of transversal (bias) fracture of specimen 5CBA-1CE/W showing a poor cellular structure in the central area.

Figure 4. SEM images showing the evolution of the cellular structure in the samples section when increasing CBA content. (Magnification: 50X).

Figure 5. Graphic summary of the cellular structure analysis in the a) section direction and b) transversal direction, containing the cell density and cell size evolution with increasing the CBA.

Figure 6. χ_m percentages for the a) first heating cycle and b) second heating cycle against relative density.

Figure 7. DSC first heating cycle-curves comparison for a) 0CBA samples; b) 1CE/A-series with increasing CBA contents from top to bottom.

Figure 8. Compression curves for 1CE/A series, showing the evolution of the behaviour when increasing the CBA amount (average standard deviations were around 8%).

Figure 9. Representation of relative compression properties: a) relative stress at the plateau σ_{pl}; b) relative stress at 25% of strain $\sigma_{25\%}$; c) relative stress at 50% of strain $\sigma_{50\%}$; against relative density. Relative refers to the properties of the foam versus the properties of the solid. The fitting lines (which follow the scaling law) have been included to guide the eye.

Figure 10. Representation of relative tensile properties: a) relative maximum strength σ_{max}; b) relative ultimate tensile strength σ_{UTS}; against relative density. Relative refers to the properties of the foam versus the properties of the solid The fitting lines (which follow the scaling law) have been included to guide the eye.

Figure 11. Impact toughness against density.

Table captions

Table 1. Composition and reference of the samples prepared (CBA=Chemical Blowing Agent; CE=Chain Extender; A=Air cooling; W=Water quenching)